GREEN'S FUNCTION AND DENSITY OF STATES OF BOUNDED P-WAVE SUPERCONDUCTORS

by
ELİT AÇILAN

Submitted to the Graduate School of Natural Sciences
in partial fulfilment of
the requirements for the degree of Master of Science

Sabancı University
October 2021

GREEN'S FUNCTION AND DENSITY OF STATES OF BOUNDED P-WAVE SUPERCONDUCTORS

Approved by:

Date of Approval: 14/10/2021

ABSTRACT

GREEN'S FUNCTION AND DENSITY OF STATES OF BOUNDED P-WAVE SUPERCONDUCTORS

Elit Açılan

Master Thesis, October 2021

Thesis Supervisor: Prof. Dr. İnanç Adagideli

Keywords: Green's functions, multiple reflection expansion, p-wave superconductors, chiral Majorana edge modes, density of states correction

In this thesis, we consider the density of states of bounded chiral p-wave superconductors, particularly focusing on the available Majorana edge modes. Majorana edge modes are among the candidates for developing structures for braiding operations and hence realizing topological quantum computers. The main aim of this thesis is to develop a novel analytical machinery to describe these Majorana edge modes in p-wave superconductors. To this end, we adopt the Multiple Reflection Expansion method developed by Balian and Bloch for the Green's function of the Helmholtz wave equation and extend this method to the Green's function of a chiral p-wave superconductor. We thus obtain an analytical expression of the Green's function near the edge of a chiral p-wave superconductor, analytically calculate the quasiparticle density of states and find signatures of the Majorana edge modes.

ÖZET

SINIRLI KİRAL P-DALGA SÜPERİLETKENLERİ İÇİN GREEN FONKSİYONU VE ENERJİ ÖZDEĞER YOĞUNLUĞU

ELIT AÇILAN

PROGRAM ADI YÜKSEK LİSANS TEZİ, EKİM 2021

Tez Danışmanı: Prof. Dr. İNANÇ ADAGİDELİ

Anahtar Kelimeler: Green fonksiyonları, çoklu yansıma açılımı, p-dalga süperiletkenler, kiral Majorana sınır modları, enerji özdeğer yoğunluğu düzeltmeleri

Bu tezde, özellikle mevcut Majorana kenar modlarına odaklanarak, sınırlı kiral p-dalgası süperiletkenlerin durumlarının yoğunluğunu ele alıyoruz. Majorana kenar modları, örgü işlemleri için yapılar geliştirmek ve dolayısıyla topolojik kuantum bilgisayarlarını gerçekleştirmek için adaylar arasındadır. Bu tezin temel amacı, p-dalgası süperiletkenlerde bu Majorana kenar modlarını tanımlamak için yeni bir analitik çerçeve geliştirmektir. Bu amaçla, Helmholtz dalga denkleminin Green fonksiyonu için Balian ve Bloch tarafından geliştirilen Çoklu Yansıma Açılımı yöntemini benimsiyoruz ve bu yöntemi iki boyutlu kiral p-dalgası süperiletkenlerin Green fonksiyonu için genişletiyoruz. Böylece, kiral p-dalgası süperiletkeninin kenarına yakın Green fonksiyonunun analitik bir ifadesini elde ediyoruz, ve yarı parçacık durum yoğunluğunu analitik olarak hesaplıyoruz ve Majorana kenar modlarının imzalarını buluyoruz.

ACKNOWLEDGEMENTS

I would like to express my gratitude to Prof. İnanç Adagideli for his endless patience and I would like to thank him for benefiting from his valuable knowledge throughout the years that I've known him. I am thankful the members of our research group, especially Dr. Ahmet Mert Bozkurt and Dr. Barış Pekerten who have guided me through my masters years. I would also like to thank my colleagues and peers in the office (dungeon, by its old name) who have supported and cheered me up during my time there. Lastly, I wish to express my sincere gratitude to my friends and my family who have always believed in me and be there for me no matter what.

TABLE OF CONTENTS

List of Figures

1 INTRODUCTION

In this thesis, we study the density of states of bounded chiral p-wave superconductors. To this end, we develop an expansion for the Green's function of chiral p-wave superconductors in two dimensions for arbitrarily shaped boundary and calculate for the case of a flat boundary. We thus extend the work of Balian and Bloch for the Helmholtz equation to the chiral p-wave superconductors. Moreover, we calculate the edge corrections to the density of states (DOS) for the flat boundary problem then analytically show the presence of chiral edge modes through the obtained spectral function.

This thesis is organized as follows. In Chapter 2, we begin by introducing the multiple reflection expansion method; here we follow the work of Balian and Bloch, the recipe of multiple reflection expansion for the Helmholtz equation. In Chapter 3, we extend the multiple reflection expansion scheme to the chiral p-wave superconductors. We first briefly introduce the topological properties of the material, the chiral p-wave superconductor, and discuss the Majorana edge modes present in the system. Then, we move on to derive the Green's function of chiral p-wave superconductor in momentum space and follow with the derivation of multiple reflection expansion for chiral p-wave superconductors. Finally, we conclude the chapter by calculating the edge corrections to the DOS and discussing the results in which we see the signatures of the previously mentioned chiral edge modes. In Chapter 4, we summarize our work and give a conclusion.

2 MULTIPLE REFLECTION EXPANSION OF THE GREEN'S FUNCTION OF THE HELMHOLTZ EQUATION

In this thesis, we adopt a powerful computation technique called multiple reflection expansion to calculate the full Green's function of a chiral p-wave superconductor, then calculate the boundary corrections to DOS by using the expansion. Therefore in this chapter, we review the method first derived for the Helmholtz equation.

Geometrical shape of the system has a considerable effect on distribution of eigenenergies in the short wavelength limit [1]. Numerical methods for calculation of eigenenergies cannot properly address to the relation between the geometric shape of the system and density of states (DOS) as much as analytical methods. Multiple reflection expansion is an analytical technique for calculating the asymptotic distribution of eigenvalues including boundary effects. This machinery can be employed in other systems as well. Therefore, we use this technique to investigate the spectral properties in an analytical fashion. Some applications of this method include graphene flakes for which Adagideli, Richter, and Würm treat various boundary cases and calculate the density of states corrections [2]. In another paper, Adagideli and Goldbart treat Andreev Billiards by using the same method [3].

Multiple reflection expansion is a series representation of the Green's Function where each term in the series represents quantum processes with a fixed number of reflections from the system boundaries. The MRE of Green's function stores the information addressing boundaries by including every possible reflection from the boundary. Using the well-known relation between Green's function and DOS, it is possible to calculate how the boundaries affect the DOS by obtaining a Green's function that includes edge corrections. To this end, in this chapter, we present a review of this

method by following Ref. [1].

In Section 2.1, we review Green's functions and their relation to DOS. In section 2.2, we introduce the multiple reflection expansion method for the Helmholtz equation.

2.1 Green's function and its relation to DOS

Multiple reflection expansion is a method that involves calculating Green's functions; therefore, we give a quick summary of Green's functions as we use Green's functions extensively in this work. In addition, we touch briefly on the relation between Green's functions and the density of states since our ultimate aim is to calculate boundary corrections to the density of states.

2.1.1 Green's functions

Green's functions correspond to the "impulse response" of a linear differential operator. Many problems in quantum mechanics can be treated analytically by finding the appropriate Green's function and imposing initial or boundary conditions according to the system [4]. Green's function as an operator is the resolvent of an eigenvalue equation such that spectral features of a system can be obtained. Therefore, the physical characteristics of a system such as DOS can be obtained by using Green's functions techniques. For a linear differential operator L, Green's function is the solution of the equation:

$$LG(x,s) = \delta(x-s), \tag{2.1}$$

where $\delta(x-s)$ is the Dirac delta function. L could be any linear differential operator such as the Laplace operator to D'alembert operator. Moreover, we can use Green's function methods to study quantum mechanical systems as Hamiltonian is a linear Hermitian operator. We define the linear differential operator $L = E - \hat{H}$. Then the Green's function for this operator satisfies the equation:

$$\left(E-\hat{H}\right)G(\mathbf{r},\mathbf{r}';E)=\delta(\mathbf{r}-\mathbf{r}'). \tag{2.2}$$

Where $\hat{H}$ is the Hamiltonian of the system. In bra-ket notation, $G(\mathbf{r},\mathbf{r}';E) = \langle\mathbf{r}|\hat{G}(E)|\mathbf{r}'\rangle$, where $\hat{G}(E)$ is the Green's function operator, a resolvent operator of an eigenvalue equation. Free space Green's function is determined by the formal inverse of $(E-\hat{H})$ as:

$$G(\mathbf{r},\mathbf{r}';E)=\left\langle\mathbf{r}\middle|\left(E-\hat{H}\right)^{-1}\middle|\mathbf{r}'\right\rangle, \tag{2.3}$$

We consider Green's function of an operator as a propagator for particles in quantum mechanics. They contain the information of probability amplitudes for a particle moving from point $\mathbf{r}$ to point $\mathbf{r}'$.

We must incorporate the boundary corrections for a bounded system to find the exact Green's function of a particular system. We can either solve the inhomogeneous by directly applying the boundary conditions or using corrections to the total Green's function by using methods such as the method of images or multiple reflection expansion. Either way, the full Green's function of a particular can then be employed for calculating the physical properties of a system such as conductance or DOS.

In the following subsection, we relate Green's functions and DOS that captures the system's physical properties.

2.1.2 Density of states

As we mentioned above the Green's function is related to the DOS [4], for completeness we provide a derivation in this section. Eigenfunctions of $\hat{H}$ form a complete set and denoted as $\phi_n(\mathbf{r})$. Both the eigenfunctions and the Green's function satisfy the same boundary conditions. In real space representation, we expand $G(\mathbf{r},\mathbf{r}';z)$ in terms of eigenfunctions as,

$$G(\mathbf{r},\mathbf{r}';z)=\sum_n\frac{\phi_n(\mathbf{r})\phi_n^*(\mathbf{r}')}{z-\lambda_n}, \tag{2.4}$$

where n represents a set of indices that may correspond to either discrete and/or

continous values. Since the Hamiltonian is a Hermitian operator, its eigenvalues denoted by λ_n are real. Moreover, $\lambda_n \neq z$ if $\mathrm{Im}\{z\} \neq 0$, which means the existing imaginary part in z implies $G(z)$ is a mesomorphic function in complex plane with simple poles on the real axis [4]. If $z = \lambda$, where λ is part of the continuous spectrum of a linear differential operator, Green's function is not well defined due to the pole in the integrand. To remedy that, we define G^+ and G^-, retarded and advanced Green's functions respectively, with $z = E \pm i\epsilon$ where ϵ is now the infinitesimal imaginary part:

$$G^{\pm}(\mathbf{r}, \mathbf{r}'; E) = \lim_{\epsilon \to 0^+} G(\mathbf{r}, \mathbf{r}'; E \pm i\epsilon). \tag{2.5}$$

The difference between $G^{\pm}$ retarded and advanced Green's functions are a set of Dirac delta functions that peak at the eigenvalues of the operator $\hat{H}$. They can also be considered as outgoing and ingoing impulses.

We integrate the Green's functions over the real-space:

$$\lim_{\epsilon \to 0^+} \int \mathrm{d}\mathbf{r}\, G(\mathbf{r}, \mathbf{r}; E \pm i\epsilon) = \lim_{\epsilon \to 0^+} \int \mathrm{d}\mathbf{r} \sum_n \frac{\phi_n(\mathbf{r})\phi_n^*(\mathbf{r})}{E - \lambda_n \pm i\epsilon}. \tag{2.6}$$

Because $\phi_n(\mathbf{r})$'s constitute a set of orthonormal function, the integral over the real-space $\int \mathrm{d}\mathbf{r}\, \phi_n(\mathbf{r})\phi_n^*(\mathbf{r}) = 1$. Then the equation above reduce to

$$\begin{aligned} \lim_{\epsilon \to 0^+} \int \mathrm{d}\mathbf{r}\, G(\mathbf{r}, \mathbf{r}; E \pm i\epsilon) &= \lim_{\epsilon \to 0^+} \sum_n \frac{1}{E - \lambda_n \pm i\epsilon} \\ &= \pm i\pi \sum_n \delta(E - \lambda_n). \end{aligned} \tag{2.7}$$

Thus we see that imaginary part of the retarded and advanced Green's functions are proportional to the density of states. We express the density of states in terms of retarded or advanced Green's functions:

$$\rho(E) = \sum_n \delta(E - \lambda_n) = \mp \frac{1}{\pi} \lim_{\epsilon \to 0^+} \mathrm{Im}\Big\{ \int \mathrm{d}\mathbf{r}\, G(\mathbf{r}, \mathbf{r}; E \pm i\epsilon) \Big\}. \tag{2.8}$$

We can compute the DOS of a system by using the equation 2.8, after finding the correct Green's function. More often than not, the critical task is to figure out the entire Green's function, including boundary corrections for a given system. One can either directly solve the inhomogeneous equation by directly imposing the boundary conditions or addressing the boundary conditions by using hypothetical sources generated by the homogenous function, the free space Green's function. For

a system with a single source, the method of images would suffice. However, we must employ multiple reflection expansion to capture numerous sources - multiple reflections. The following section reviews the multiple reflection expansion method for the Helmholtz equation.

2.2 Multiple reflection expansion of the Green's function of the Helmholtz equation

The study of the distribution of eigenvalues is a helpful tool to understand the physics properties of a system in many areas of physics. Balian and Bloch treated the problem of distribution of eigenfrequencies for the Helmholtz equation in their remarkable papers beginning from 1970 [1]. They used a time-independent Green's function method amd developed a technique called multiple reflection expansion, which is the main tool of this thesis. In the small wavelength limit compared to the typical dimension of the system, distribution of eigenergies or density of states can be calculated with this method.

The treatment of the Helmholtz equation begins by determining the Green's function of the system. The equation we consider is,

$$(\boldsymbol{\nabla}^2 + k^2)\Psi = 0, \tag{2.9}$$

where Ψ is the wave function, and k is the wavenumber.

First, we consider the free space Green's function, sometimes called homogenous solution of this equation. We identify $\boldsymbol{\nabla}^2 + k^2$ to be the linear differential operator, and we refer it as L in this section. Thus the Green's function of this operator solves the equation (2.1). Green's functions can be represented in terms of eigenfunctions of the relevant operator as shown in equation (2.4). The eigenfunctions of this linear differential operator, ϕ_n, are known to be plane waves. Using the aforementioned orthonormal plane wave functions, we obtain the free space Green's function by changing sum to an integral in momentum space as

$$G_0(\mathbf{r}, \mathbf{r}'; E + i\epsilon) = \int \frac{\mathrm{d}^3 k}{(2\pi)^3} \frac{e^{-i\mathbf{k}\cdot(\mathbf{r}'-\mathbf{r})}}{k^2 - E - i\epsilon}. \tag{2.10}$$

The integral can be carried out in the complex plane by the residue theorem, where we evaluate the simple pole in the integrand. We thus find the homogenous Green's function of the Helmholtz equation in three dimensions:

$$G_0(\mathbf{r},\mathbf{r}') = \frac{e^{ik|\mathbf{r}-\mathbf{r}'|}}{4\pi|\mathbf{r}-\mathbf{r}'|} \tag{2.11}$$

Note that square root of $E+i\epsilon$ with the positive imaginary part is denoted by k. Now that we determine the free space Green's function of the Helmholtz equation, we move on to investigate the edge effects in the next section.

2.2.1 Parametrizing Green's function

The free space Green's function $G_0(\mathbf{r},\mathbf{r}';E)$, governs the particle dynamics in the bulk of a system. However we must parametrize it to address the boundary effects. The Green's function satisfies the relation for the entire space.

$$(E-\hat{L})G_0(\mathbf{r},\mathbf{r}';E) = \delta(\mathbf{r}-\mathbf{r}'). \tag{2.12}$$

However, in order to find the *full* Green's function of a bounded region, we must impose the boundary conditions for the system under question. We can approximately construct the full Green's function from the free space Green's function of the system by method of images [5].

For a system with a flat boundary, we place an imaginary "charge" outside of the physical boundary so that the "field" of both charges satisfies the correct boundary conditions. Then the overall problem with boundaries is now expressed in terms of as a sum of Green's function with the initial and image charges. Essentially, the added image charge enocdes the effect of the boundary conditions. To clarify, let $\mathbf{r}'$ be a point inside the boundary and its mirror image with respect to the flat boundary $\mathbf{r}'_{image}$. Then the full Green's function of the system satisfying the boundary conditions given by:

$$G(\mathbf{r},\mathbf{r}') = G_0(\mathbf{r},\mathbf{r}') \pm G_1(\mathbf{r},\mathbf{r}'_{image}) \tag{2.13}$$

We introduced the auxiliary Green's function $G_1(\mathbf{r},\mathbf{r}'_{image})$ as the correction term

that imposes the boundary conditions to express full Green's function $G(\mathbf{r}, \mathbf{r}')$.

However, the method of images fails to address possible multiple sources; it only works for a singular source. Thus, we need to use a method to embody more than one source. The next section introduces an idea borrowed from the potential theory to capture the multiple sources as multiple reflections.

2.2.2 Correction to Green's function due to multiple sources

As mentioned above, we must employ a different method to address multiple sources for an inhomogeneous equation. To this end, we use a technique from potential theory to incorporate the various sources to determine the full Green's function of a system. We express the multiple sources as a potential function in terms of an unknown charge (or dipole) layer on the boundary [6]. In general, the correction term G_1 can be expressed as a double layer potential, as a result of a double layer potential on the boundary:

$$G_1 = \int_{\partial V} \mathrm{d}\sigma_\alpha \frac{\partial G_0(\mathbf{r}, \boldsymbol{\alpha})}{\partial \mathbf{n}_\alpha} \mu(\boldsymbol{\alpha}, \mathbf{r}'), \tag{2.14}$$

where μ is yet an unknown surface dipole density function, and the derivative of G_0 is taken normal to the surface, and the integral is over the boundary points $\boldsymbol{\alpha}$. The boundary integral expression with the unknown density function is the correction due to "multiple sources". Together with the correction term, we express the full Green's function in terms of G_0 as:

$$G(\mathbf{r}, \mathbf{r}') = G_0(\mathbf{r}, \mathbf{r}') - \int_{\partial V} \mathrm{d}\sigma_\alpha \frac{\partial G_0(\mathbf{r}, \boldsymbol{\alpha})}{\partial \mathbf{n}_\alpha} \mu(\boldsymbol{\alpha}, \mathbf{r}'). \tag{2.15}$$

In this thesis, we reserve the Greek letters such as $\boldsymbol{\alpha}$ for the points on the boundary. The correction term is an integral only defined on the boundary. G_0 is the Green's function given by the equation (2.11). We must first determine the unknown dipole density function, and then we can obtain the expression for the total Green's function of the system.

The equation (2.15) is the starting point of derivation of multiple reflection expansion. By applying the boundary conditions, we can find a self-consistent relation for the dipole density function, generating the full Green's function by iteratively re-

placing the dipole density function μ with the obtained relation. In turn, we obtain an integral series. In the next subsection, we show how we incorporate the boundary conditions and find the relation for μ, thereby obtaining the expansion for the full Green's function.

2.2.3 Parameterization of the Green's function in the presence of a boundary

Until now, we managed to express the total Green's function in terms of the free space Green's function and a double layer potential (a boundary integral with functions including G_0 and the unknown surface dipole density function μ given by the equation (2.15)). We consider the Dirichlet boundary conditions for this problem, that if $\mathbf{r}$ is a point on the boundary, that is $\mathbf{r} = \boldsymbol{\beta}$, the the Green's function must vanish.

We start by considering the case of a smooth boundary in three-dimensional space. We take two points on the boundary surface; one is a fixed point that $\mathbf{r}$ approaches to, which we call $\boldsymbol{\beta}$. Moreover, another point on the surface $\boldsymbol{\alpha}$ denote the integral variable in the integral. The boundary conditions dictate that

$$\lim_{\mathbf{r}\to\boldsymbol{\beta}} G(\mathbf{r},\mathbf{r}') = G_0(\boldsymbol{\beta},\mathbf{r}') + \lim_{\mathbf{r}\to\boldsymbol{\beta}} \int \mathrm{d}\sigma_\alpha \frac{\partial G_0(\mathbf{r},\boldsymbol{\alpha})}{\partial \mathbf{n}_\alpha} \mu(\boldsymbol{\alpha},\mathbf{r}') = 0. \tag{2.16}$$

While the limit of the first term is easy to determine, the limit of the next term - the boundary integral is cumbersome as the integrand is singular where the two points on the boundary coincide, that is $\boldsymbol{\beta} = \boldsymbol{\alpha}$, due to the short range singular nature of G_0. Therefore, we divide the integration region into two parts, one containing the singularity, and the other being free of singularity.

The domain of D_δ consists of points $\boldsymbol{\alpha} \in \partial V$, such that $|\boldsymbol{\beta} - \boldsymbol{\alpha}| < \delta$ encompassing the singular point $\boldsymbol{\beta} = \boldsymbol{\alpha}$. The domain of $\bar{D}_\delta$ is the rest of the points on the boundary where the integramd is not singular. After performing the integration, we can take the limit $\delta \to 0$.

The boundary integral in separated domains is

$$\lim_{\mathbf{r}\to\boldsymbol{\beta}} \int_{D_\delta} \mathrm{d}\sigma_\alpha \frac{\partial G_0(\mathbf{r},\boldsymbol{\alpha})}{\partial \mathbf{n}_\alpha} \mu(\boldsymbol{\alpha},\mathbf{r}') + \lim_{\mathbf{r}\to\boldsymbol{\beta}} \int_{\bar{D}_\delta} d\sigma_\alpha \frac{\partial G_0(\mathbf{r},\boldsymbol{\alpha})}{\partial \mathbf{n}_\alpha} \mu(\boldsymbol{\alpha},\mathbf{r}'). \tag{2.17}$$

Assuming μ is a slow-changing function over the domain D_δ, we can take out of the integral. The remaining part of the integrand produces the result $\frac{1}{2}$, then the integral over the singular part is

$$\lim_{\mathbf{r}\to\boldsymbol{\beta}} \int_{D_\delta} \mathrm{d}\sigma_\alpha \frac{\partial G_0(\mathbf{r},\boldsymbol{\alpha})}{\partial \mathbf{n}_\alpha} \mu(\boldsymbol{\alpha},\mathbf{r}') = \frac{1}{2}\mu(\boldsymbol{\beta},\mathbf{r}'). \tag{2.18}$$

We evaluate the limit of non-singular part given in the equation (2.17), and then we obtain the self-consistency relation for the unknown surface dipole density function:

$$\frac{1}{2}\mu(\boldsymbol{\beta},\mathbf{r}') = -G_0(\boldsymbol{\beta},\mathbf{r}') - \int_{\partial V} \mathrm{d}\sigma_\alpha \frac{\partial G_0(\boldsymbol{\beta},\boldsymbol{\alpha})}{\partial \mathbf{n}_\alpha} \mu(\boldsymbol{\alpha},\mathbf{r}'). \tag{2.19}$$

This equation for μ is nonsingular and uniquely define μ. This equation can be solved by iteration if the surface is smooth enough.

2.2.4 Reflections from boundaries

We expressed the full Green's function in terms of G_0 and a boundary integral consisting of $\frac{\partial G_0}{\partial \mathbf{n}_\alpha}$ and an unknown dipole density function μ. In addition, we obtained the self-consistency relation for the unknown density function μ. We acquire an integral series for the entire Green's function G by combining two expressions. We first obtain a solution for the self-consistency relation by iteration. This produces an integral series for μ.

$$\begin{aligned}\mu(\boldsymbol{\alpha},\mathbf{r}') = -2G_0(\boldsymbol{\alpha},\mathbf{r}') + 2^2 \int_{\partial V} \mathrm{d}\sigma_\beta \frac{\partial G_0(\boldsymbol{\alpha},\boldsymbol{\beta})}{\partial \mathbf{n}_\beta} G_0(\boldsymbol{\beta},\mathbf{r}') \\ - 2^3 \int_{\partial V} \mathrm{d}\sigma_\beta \, \mathrm{d}\sigma_\gamma \frac{\partial G_0(\boldsymbol{\alpha},\boldsymbol{\beta})}{\partial \mathbf{n}_\beta} \frac{\partial G_0(\boldsymbol{\beta},\boldsymbol{\gamma})}{\partial \mathbf{n}_\gamma} G_0(\boldsymbol{\gamma},\mathbf{r}') + \dots .\end{aligned} \tag{2.20}$$

Each iteration produces a new term and extends the integral series, generating a new reflection term. We stress that all the terms now only depend on the function G_0. Now, we substitute this expansion into the equation (2.15), to replace the term μ in the boundary integral. As a result, we achieve an expansion where each term represents the corrections as reflections from boundaries and obtain the full Green's function:

$$G(\mathbf{r},\mathbf{r}') = G_0(\mathbf{r},\mathbf{r}') - 2\int_{\partial V} \mathrm{d}\sigma_\alpha \frac{\partial G_0(\mathbf{r},\boldsymbol{\alpha})}{\partial \mathbf{n}_\alpha} G_0(\boldsymbol{\alpha},\mathbf{r}') + 2^2 \int_{\partial V} \mathrm{d}\sigma_\alpha \int_{\partial V} \mathrm{d}\sigma_\beta \frac{\partial G_0(\mathbf{r},\boldsymbol{\alpha})}{\partial \mathbf{n}_\alpha} \frac{\partial G_0(\boldsymbol{\alpha},\boldsymbol{\beta})}{\partial \mathbf{n}_\beta} G_0(\boldsymbol{\beta},\mathbf{r}') - \dots \quad (2.21)$$

Each term in the expansion represents a fixed number of reflections from the edges. Hence the sum is named as multiple reflection expansion. For example, the first term, the free space Green's function corresponds to the path between $\mathbf{r}$ and $\mathbf{r}'$. The second term signifies the path connecting $\mathbf{r}$ and $\mathbf{r}'$ with $\boldsymbol{\alpha}$ inbetween, the path in total corresponds to one reflection off the boundary. The next term includes two reflections from boundary and so on. Thus, we interpret the sum as all the quantum paths from $\mathbf{r}$ to $\mathbf{r}'$ with reflection points on $\boldsymbol{\alpha}$, $\boldsymbol{\beta}$, $\boldsymbol{\gamma}$ and more.

We thus derive the full Green's function G as an expansion including all possible reflections from the edges. We stress that the expansion (2.21) for the full Green's function is convergent for $\epsilon > 0$ and finite system. We can unearth the information it contains, such as conductance using the Fisher-Lee relation or the density of states using the relation is given in equation (2.8).

Balian and Bloch calculated the surface contributions to the density of states for the Helmholtz equation in three dimensions by using the plane approximation, taking two dimensional Fourier transform along the plane, assuming approximate translational invariance along the boundary. They also calculated the curvature contribution by other approximations [1].

In this chapter, we introduced the method of multiple reflection expansion by following Ref [1]. We reviewed the derivation of total Green's function of Helmholtz equation for smooth boundaries. We arrived at the expansion, which we identified as a sum of quantum paths connecting two arbitrary points inside of the region $\mathbf{r}$ and $\mathbf{r}'$, with a fixed number of reflections off the boundary points $\boldsymbol{\alpha}$, $\boldsymbol{\beta}$, $\boldsymbol{\gamma}$.

In the next chapter, we will adopt the scheme to treat the chiral p-wave superconductor in two dimensions with a flat boundary to derive the expansion. We will also use the expansion to calculate the edge corrections to the density of states.

3 MULTIPLE REFLECTION EXPANSION FOR BOUNDED CHIRAL P-WAVE SUPERCONDUCTORS

In the present chapter, we will extend the multiple reflection expansion method we reviewed in the previous chapter to investigate gapless chiral Majorana modes of a bounded p-wave superconductor in two dimensions. In particular, we calculatethe edge corrections to the Green's function, which in turn we use to calculate the edge corrections to the density of states. The spectral function we obtain exhibits the signatures of a Majorana mode, and thereby we demonstrate the presence of Majorana modes in chiral p-wave superconductors analytically. Although it is well known that this system hosts Majorana modes along the boundary, we derive analytic expression for the exact Green's function, which to our knowledge was not known.

In this chapter, we first focus on the chiral p-wave superconductors, a topologically non-trivial phase that can host the aforementioned Majorana modes. We derive a Green's function method to examine its properties analytically. In other words, we extend the multiple reflection expansion method for the chiral p-wave superconductors to determine the edge corrections to the DOS, thereby presenting the Majorana edge modes stemming from the non-trivial topology of chiral p-wave superconductors.

We organize the present chapter in this order: In section 3.1, we first introduce the chiral p-wave superconductors and emphasize the existence of one-dimensional edge modes known as Majorana modes that arise due to the symmetries and dimensionality of the system. In section 3.2, we derive the multiple reflection expansion for the Green's function of a two-dimensional bounded chiral p-wave superconductor. In section 3.3, for a flat boundary, we calculate the full edge contributions to the Green's function, thus obtaining the exact Green's function. Additionally, we dis-

cuss the result in the context of edge modes present in the two-dimensional p-wave superconductors.

3.1 Chiral p-wave Superconductors

Topological p-wave superconductor is one of the topologically non-trivial phases of matter, which are bulk quasiparticle insulators that are characterized by a bulk non-zero topological number and host gapless edge states [7]. It is an unconventional type of superconductor in which the Cooper pairs are in triplet pairing state [8]. As part of the topological family, the bulk spectrum of a p-wave topological superconductor also feature an energy gap and gapless Majorana edge states [9].

These edge modes are unique because they are unaffected by defects or disorders, consequently are topologically protected and robust. Topological p-wave superconductor edge modes are chiral. This means that the edge modes allow motion in only one direction hence there are no available states for backscattering. The direction of the motion is opposite for opposite edges.

Chiral p-wave superconductors are part of symmetry class D [10]. From a theoretical standpoint, symmetry class D, that is, particle-hole symmetry present and time-reversal symmetry broken, there exists $\mathbb{Z}$ classification for a one-dimensional boundary in two dimensions that host gapless edge states [11]. Their Chern number, a topological invariant related to the presence of edge states in a system in a way that the Chern invariant is equal to the difference between the number of right moving and left moving modes, classifying $\mathbb{Z}$ suggests the existence of edge modes. While the Chern number is a bulk property, due to bulk-boundary correspondence, the nontrivial bulk topology leads to the topologically protected edge states at the boundaries of the system [12].

Topological superconductors may host Majorana *zero* modes at the cores of vortices in two dimensions [13, 14] and at the ends of superconducting quantum wires [15]. The Majorana zero modes have non-Abelian exchange statistics allowing them to be a candidate for realizing topological quantum computation [16]. However, these bound states are immobile, and their exchange cannot be demonstrated in real space. There exist proposals addressing the immobility of bound states by utilizing the chiral Majorana edge modes together with the aforementioned Majorana zero modes that can work in real-space [17]. Thus the chiral Majorana edge modes are

equally crucial for realizing topological quantum computers.

There are several material proposals for chiral p-wave superconductors. For example, due to the spin-degenerate Fermi surface due to Ru, Sr_2RuO_4 is a candidate material for realizing the p-wave superconductivity at low temperatures [18, 19], one of the other proposals that resemble a chiral p-wave superconductor without breaking time-reversal symmetry include a hybrid system where conventional superconductors with s-wave pairing are used to induce superconductivity on the surface of a topological insulator by proximity effect [20]. In addition, there are many proposed experiments for spotting the Majorana signatures in p-wave superconductors, such as Josephson effects experiments [21], tunneling measurements [22], and interferometry measurements [23]. Main focus in this work is analytical, we refer the reader to Refs. [24, 7, 25, 26, 11] for further discussion in materials and experiments and an extended review.

The quasiparticle dynamics in a chiral p-wave superconductor is governed by the Hamiltonian:

$$\hat{H} = (\frac{p^2}{2m} - \mu)\sigma_3 + \Delta \mathbf{p} \cdot \boldsymbol{\sigma}, \tag{3.1}$$

where $\mathbf{p} = (p_x, p_y)$ is momentum, Δ stands for the superconducting pairing potential, μ stands for chemical potential, $\boldsymbol{\sigma} = (\sigma_x, \sigma_y, \sigma_z)$ are Pauli matrices acting in the particle-hole space. The second term in equation (3.1) describes a p-wave type pairing: the superconducting pairing Δ is proportional to $\mathbf{p}$. We can consider this Hamiltonian to be a two-dimensional generalization of the Kitaev chain that has a similar linear term in one dimension [15]. Moreover, this linear component of the Hamiltonian breaks the time-reversal symmetry and leads to a non-zero Chern number, thus leading to topologically non-trivial behavior [7].

The bulk energy spectrum of chiral superconductors is given by,

$$E = \pm\sqrt{(\frac{k^2}{2} - \mu)^2 + \Delta^2 k^2} \tag{3.2}$$

note that we take $\hbar = m = 1$. The excitation spectrum is plotted in Fig. 3.1 for $\mu = -1.5t$, $\mu = 0$, $\mu = 1.5t$ respectively, with $\Delta = 0.5t$, where $t = \frac{\hbar^2}{2ma^2}$, and we set the typical unit length a to unity. We note that the bulk spectrum is gapped as expected.

As the energy gap closes, we see that topological phase transition occurs at $\mu = 0$. We deduce from the plots that topological phase transition occurs when $\mu = 0$ as

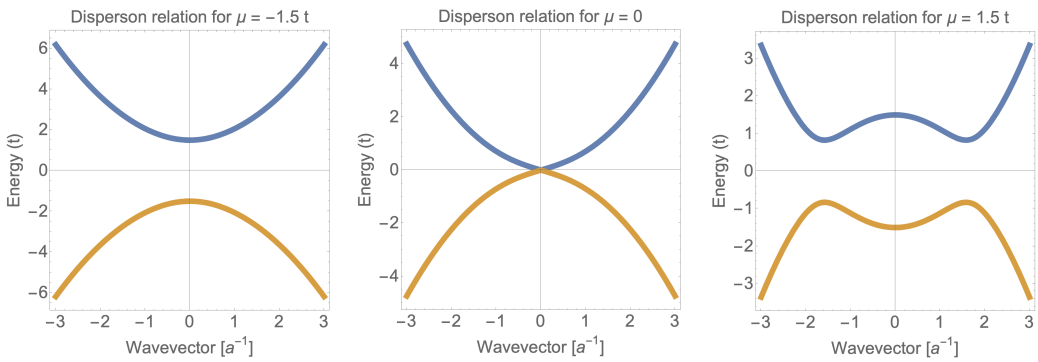

(a) $\mu = -1.5t$ (b) $\mu = 0$ (c) $\mu = 1.5t$

Figure 3.1 Dispersion relation for different μ values, displaying the distinct topological phases for $\Delta = 0.5t$

we see that the gap is closed. The band structures of $\mu > 0$ and $\mu < 0$ are gapped. However, $\mu > 0$ is a topologically non-trivial phase with gapless edge modes, whereas there is no gapless edge mode when $\mu < 0$ as we shall see in the next section.

In the next section, we derive the multiple reflection expansion for p-wave superconductors and calculate the edge corrections for a flat boundary that captures non-trivial behavior and the Majorana edge mode and distinguishes between the two distinct phases.

3.2 Multiple reflection expansion of the Green's function of bounded

p-wave chiral superconductors

As demonstrated in Chapter 2, the multiple reflection expansion method is an effective tool to derive a full Green's function of a system. The total Green's function can be viewed as a sum of all quantum processes involving reflections from the boundaries such that it captures the boundary information. It is an integral series whose terms are related to the density of states. Thus the expansion provides a framework to calculate the edge corrections to the DOS, a spectral function encompassing the signatures of Majorana modes.

In this section, we calculate the full Green's function by the multiple reflection expansion method for a flat boundary in two dimensions. We follow the same recipe reviewed in Chapter 2 in Ref [1]; however, the Hamiltonian is now that of a chiral p-wave superconductor, and we focus on a smooth one-dimensional boundary of

a two-dimensional system rather than the two-dimensional planar boundary of a three-dimensional system.

In this section, we first begin with deriving the Green's function given in momentum space. Then, we parametrize the Green's function near the boundary by using the potential theory. Next, we obtain a self-consistent expression for the dipole density function and obtain the expansion. We briefly discuss Weyl's expansion and relate its terms to Green's functions. Finally, we work out a spectral function amounting to the edge corrections to the density of states of chiral p-wave superconductors for a smooth boundary in two dimensions. We present the plots of spectral functions and discuss the features present in this system.

3.2.1 Green's function of a chiral p-wave superconductor

We obtain the full Green's function of a chiral p-wave superconductor by multiple reflection expansion method. We first obtain the free space Green's function. We do this by first finding the Green's function in momentum representation for the Hamiltonian given by the equation (3.1). The Green's function satisfies the relation:

$$\left(\hat{H} - E\sigma_0\right) G_0(\mathbf{r}, \mathbf{r}'; E) = \frac{\hbar^2}{2m}\delta(\mathbf{r} - \mathbf{r}'), \tag{3.3}$$

where $\mathbf{r}$ and $\mathbf{r}'$ are points in space, $\hbar$ is the Planck's constant and $\delta(\mathbf{r} - \mathbf{r}')$ is the Dirac delta function. Here we note that $\left(\hat{H} - E\sigma_0\right)$ is a 2×2 matrix valued operator, consequently the free space Green's function $G_0(\mathbf{r}, \mathbf{r}'; E)$ here is a 2×2 matrix valued function where σ_0 is the identity matrix. We first define $\mathbf{k} = \frac{\mathbf{p}}{\hbar}$, $k_\alpha = \frac{m\Delta}{\hbar}$, $\bar{\mu} = \frac{2m\mu}{\hbar^2}$, $\bar{E} = \frac{2mE}{\hbar^2}$ and in line with the previous chapter, we express the Green's function as a formal inverse of the operator $\left(\hat{H} - \bar{E}\sigma_0\right)$ in momentum space:

$$G_0(\mathbf{k}; \bar{E}) = \left((k^2 - \bar{\mu})\sigma_3 + k_\alpha \mathbf{k} \cdot \boldsymbol{\sigma} - \bar{E}\sigma_0\right)^{-1}. \tag{3.4}$$

We now multiply both the denominator and the numerator by $\left(\bar{E}\sigma_0 + \hat{H}(\mathbf{k})\right)$. Using the method of partial fractions, we write the denominator in ters of familiar Green's functions of the scalar wave equation,

$$G_0(\mathbf{k};\bar{E}) = \frac{\bar{E}\sigma_0 + 2k_\alpha \mathbf{k}\cdot\boldsymbol{\sigma} - 2k_\alpha^2\sigma_3}{k_+^2 - k_-^2}\left(\frac{1}{k^2-k_+^2} - \frac{1}{k^2-k_-^2}\right) + \frac{1}{2}\sigma_3\left(\frac{1}{k^2-k_+^2} + \frac{1}{k^2-k_-^2}\right) \tag{3.5}$$

Where $k_\pm^2 = \mu - 2k_\alpha^2 \pm \sqrt{4k_\alpha^4 - 4\mu k_\alpha^2 + \bar{E}^2}$. We note that due to presence of $\bar{E}$, $k_\pm$ has opposite imaginary parts which leads to retarded and advanced scalar Green's functions respectively.

The Green's function given by the equation (3.5) is represented in momentum space. We evaluate the Fourier transformation in order to obtain the real-space Green's function. The real-space Green's function can then be utilized to determine the bulk density of states of a system. In this section, we focus on a bounded region. In order to enforce the boundary conditions satisfied by the Green's function, we extend the multiple reflection expansion method and obtain an analytic expression for the full Green's function.

3.2.2 Parameterization of the p-wave superconductor Green's function

We are interested in a system with a boundary, however the free space Green's function only reveals bulk information. We derive an analytic expression for Green's function of a chiral p-wave superconductor by multiple reflection expansion that incorporates the edge effects as well.

We start by parametrizing the Green's function near a boundary. We eco the same steps in Chapter 2, and begin by defining an auxiliary Green's function as a double potential - a boundary integral by potential theory [6] with yet unknown dipole layer density function $\mu(\boldsymbol{\alpha},\mathbf{r}')$. Then we express the full Green's function as a sum of free space and auxiliary Green's functions:

$$G(\mathbf{r},\mathbf{r}') = G_0(\mathbf{r},\mathbf{r}') - \int_{\partial S} \mathrm{d}\sigma_\alpha \frac{\partial G_0(\mathbf{r},\boldsymbol{\alpha})}{\partial \mathbf{n}_\alpha}\mu(\boldsymbol{\alpha},\mathbf{r}') \tag{3.6}$$

where the integral is over the boundary denoted by ∂S and $\boldsymbol{\alpha} \in \partial S$ signifies a point residing on the boundary. Note that, G, G_0 and μ are all 2×2 matrix-valued functions. We parametrized G_0 by the matrix function μ including the boundary corrections with the same technique that was used by Balian and Bloch as well as Adagideli and Goldbart [1, 3].

Now, to parametrize we investigate the asymptotic behavior near the boundary. For that, we first start by applying Dirichlet boundary conditions where the function vanishing on the boundary. Thus, the full Green's function is vanishing in the asymptotic limit $\mathbf{r}$ goes to $\boldsymbol{\beta}$,

$$\lim_{\mathbf{r}\to\boldsymbol{\beta}} G(\mathbf{r},\mathbf{r}') = G_0(\boldsymbol{\beta},\mathbf{r}') + \lim_{\mathbf{r}\to\boldsymbol{\beta}} \int \mathrm{d}\sigma_\alpha \frac{\partial G_0(\mathbf{r},\boldsymbol{\alpha})}{\partial \mathbf{n}_\alpha} \mu(\boldsymbol{\alpha},\mathbf{r}') = 0. \tag{3.7}$$

Again, the integral in the boundary integral is singular in this limit. Therefore, we must evaluate the integral by separating the singular and non-singular parts in the same fashion in Chapter 2, following Ref. [3].

We separate the domain of integration into two segments D_δ and $\bar{D}_\delta$. The domain of D_δ consists of points on the boundary of surface S $\boldsymbol{\alpha} \in \partial S$, such that $|\boldsymbol{\beta} - \boldsymbol{\alpha}| < \delta$ encompassing the singular point $\boldsymbol{\beta} = \boldsymbol{\alpha}$. The domain of $\bar{D}_\delta$ is the rest of the points on the boundary where the integral is not singular, $\bar{D}_\delta = \partial S / D_\delta$. After separating the domain of integration, we can take the limit $\delta \to 0$. Now, in this limit boundary integral is equal to

$$\lim_{\mathbf{r}\to\boldsymbol{\beta}} \int_{D_\delta} \mathrm{d}\sigma_\alpha \frac{\partial G_0(\mathbf{r},\boldsymbol{\alpha})}{\partial \mathbf{n}_\alpha} \mu(\boldsymbol{\alpha},\mathbf{r}') + \lim_{\mathbf{r}\to\boldsymbol{\beta}} \int_{\bar{D}_\delta} d\sigma_\alpha \frac{\partial G_0(\mathbf{r},\boldsymbol{\alpha})}{\partial \mathbf{n}_\alpha} \mu(\boldsymbol{\alpha},\mathbf{r}'). \tag{3.8}$$

Near the boundary where the distance $|\mathbf{r} - \mathbf{r}'|$ tends to zero, we can use the limiting expression for the Green's function. We take the inverse Fourier transformation of $G_0(\mathbf{k})$ and obtain the Green's function in real-space representation. We find that Fourier transformation of $\frac{1}{k^2 - k_\pm^2}$ is zeroth order Hankel function of the first kind with spatial variables in two dimensions, that is $\pm\frac{i}{4} H_0^\pm(k_\pm|\mathbf{r} - \mathbf{r}'|)$ where $\mathrm{Re}\{k_\pm\} > 0$ [27].

Furthermore, in the limit where $|\mathbf{r} - \mathbf{r}'|$ tends to 0, the asymptotic form of $H_0^\pm$is $\pm\frac{2i}{\pi}\ln(|\mathbf{r} - \mathbf{r}'|)$. In this limit, only the term proportional to σ_3 contributes as the other components cancel out. Finally, asymptotically $G_0(|\mathbf{r} - \mathbf{r}'|)$ become $\frac{1}{2\pi}\sigma_3 \ln(|\mathbf{r} - \mathbf{r}'|)$. Now we calculate the singular part while assuming that the unknown density function is slowly changing over the range of δ as $|\delta| \to 0$ where $\boldsymbol{\alpha}$ is in very close proximity to $\boldsymbol{\beta}$. We evaluate the singular part of the integral:

$$\lim_{\mathbf{r}\to\boldsymbol{\beta}} \int_{D_\delta} \mathrm{d}\sigma_\alpha \frac{\partial G_0(\mathbf{r},\boldsymbol{\alpha})}{\partial \mathbf{n}_\alpha} \mu(\boldsymbol{\alpha},\mathbf{r}') = \frac{1}{2}\sigma_3 \mu(\boldsymbol{\beta},\mathbf{r}'). \tag{3.9}$$

Finally, we determine the expression for the dipole density function after evaluating the limit of the non-singular integral and arranging the terms in equation (3.7).

$$\frac{1}{2}\sigma_3\mu(\boldsymbol{\beta},\mathbf{r}') = -G_0(\boldsymbol{\beta},\mathbf{r}') - \int \mathrm{d}\sigma_\alpha \frac{\partial G_0(\boldsymbol{\beta},\boldsymbol{\alpha})}{\partial \mathbf{n}_\alpha}\mu(\boldsymbol{\alpha},\mathbf{r}'). \tag{3.10}$$

This is an inhomogenous integral equation, we obtain the solution by iteration:

$$\sigma_3\mu(\boldsymbol{\beta},\mathbf{r}') = -2G_0(\boldsymbol{\beta},\mathbf{r}') + (-2)^2 \int \mathrm{d}\sigma_\alpha \frac{\partial G_0(\boldsymbol{\beta},\boldsymbol{\alpha})}{\partial \mathbf{n}_\alpha}\sigma_3 G_0(\boldsymbol{\alpha},\mathbf{r}') + \dots \tag{3.11}$$

Then, we substitute the infinite series of integrals into (3.6). As a result, we generate an integral series that consists of solely free-space Green's function and its normal derivative:

$$\begin{aligned} G(\mathbf{r},\mathbf{r}') = G_0(\mathbf{r},\mathbf{r}') - 2\int_{\partial S} \mathrm{d}\sigma_\alpha \frac{\partial G_0(\mathbf{r},\boldsymbol{\alpha})}{\partial \mathbf{n}_\alpha}\sigma_3 G_0(\boldsymbol{\alpha},\mathbf{r}') \\ + 2^2 \int_{\partial S} \mathrm{d}\sigma_\alpha\, \mathrm{d}\sigma_\beta \frac{\partial G_0(\mathbf{r},\boldsymbol{\alpha})}{\partial \mathbf{n}_\alpha}\sigma_3 \frac{\partial G_0(\boldsymbol{\alpha},\boldsymbol{\beta})}{\partial \mathbf{n}_\beta}\sigma_3 G_0(\boldsymbol{\beta},\mathbf{r}') - \dots \end{aligned} \tag{3.12}$$

As was the case in the previous Chapter, the full Green's function derived by multiple reflection expansion method encapsulates the reflections from the edges. The total Green's function is interpreted as a sum of quantum paths from $\mathbf{r}$ to $\mathbf{r}'$ with reflections off of points on the boundary $\boldsymbol{\alpha}$, $\boldsymbol{\beta}$, $\boldsymbol{\gamma}$ and so on. While the recipe and the ideas behind both multiple reflection expansion are the same, the main differences between (2.21) and (3.12) is that latter has the Pauli matrix σ_3 for every reflection and the present free-space Green's function is of that of a chiral p-wave superconductor, which is a 2×2 matrix.

3.2.3 The edge corrections to the DOS

The Weyl expansion [28] is an expansion for the density of states in powers of $\frac{\lambda}{L}$ where λ is the de Broglie wavelength of the particle, and L is the linear size of the system. The terms in Weyl expansion corresponds to different geometrical sizes. The relation between the density of states and Green's functions implies that the multiple reflection expansion is closely related to the Weyl Expansion. The expansion is given by:

$$\rho(E) = \sum_n \rho_n(E) \tag{3.13}$$

The expression for the multiple reflection expansion consists of zero-reflection and one reflection from the edge and more. The first term in the expansion $G_0(\mathbf{r}, \mathbf{r}')$ is the zero-reflection propagation of the quasiparticles. The first term $\rho_0(E)$ in the Weyl expansion is the bulk term that depends on the system's bulk volume, and it is determined by the free space (or zero-reflection) Green's function. There is a one-to-one correspondence with Weyl expansion terms and multiple reflection expansion terms for scalar wave equation. The density of states terms can be derived from the multiple reflection expansion terms by the relation given in the (2.8).

Denoting the total contribution to the density of states by$\rho(E)$, we can single out the boundary contributions to the density of states as:

$$\delta\rho = \rho(E) - \rho_0(E). \tag{3.14}$$

Using the relation (2.8), the free-space Green's function and the bulk density of states $\rho_0(E)$ are related as well as the total density of states $\rho(E)$ and the total Green's function are similarly related. Therefore, that leaves the edge contribution to DOS information to the boundary integral, the correction term G_1 described by a double layer potential. If we substitute the full Green's function given by the equation (3.6) into the relation (2.8), we would get the total density of states given in (3.13). If we substract the free space Green's function part corresponding to the bulk DOS, we acquire the boundary corrections to the DOS given in the equation (3.14):

$$\delta\rho(E) = -\frac{1}{\pi}\,\mathrm{Im}\left\{\mathrm{Tr}\int_{\partial S} \mathrm{d}\sigma_\alpha \frac{\partial G_0(\mathbf{r}, \boldsymbol{\alpha}; E + i\epsilon)}{\partial \mathbf{n}_\alpha} \mu(\boldsymbol{\alpha}, \mathbf{r}'; E + i\epsilon)\right\}. \tag{3.15}$$

We note that we assume that energy has an infinitesimal imaginary part $E \to E + i\epsilon$ and trace now includes a sum over Pauli matrices as G_0 and μ are 2×2 matrices, unlike the case in Chapter 2.

The equation (3.15) represents the boundary corrections to the density of states and is central to this thesis. In the next section, we calculate this spectral function for a chiral p-wave superconductor in two dimensions with a flat boundary.

3.3 Calculation of edge corrections to the DOS of chiral p-wave superconductors

In the previous section, we obtained the boundary contributions to the density of states in equation (3.15). We now assume a flat boundary for the system in this section. This assumption allows us to define partial Fourier transform along the flat boundary. That is analogous to the plane approximation in Refs. [1, 2].

Partial Fourier transform is defined along the boundary assuming the boundary is flat. For an arbitrary function $f(\mathbf{k})$ the partial Fourier transform is defined as

$$f(k_x, y-y') = \int \frac{\mathrm{d}k_y}{2\pi} e^{ik_y(y-y')} f(\mathbf{k}) \tag{3.16}$$

We refer the reader to the appendix for details of partial Fourier transformation of each expression.

For a flat boundary, we obtain the expression for the edge correction to the DOS:

$$\delta\rho_{k_x}(E) = -\frac{1}{\pi}\mathrm{Im}\left\{\mathrm{Tr}\int_0^\infty \mathrm{d}y\, \frac{\partial G_0(k_x, y'-y)}{\partial y'}\bigg|_{y'=y_\alpha} \mu(k_x, y-y_\alpha)\right\}. \tag{3.17}$$

Now, we will obtain the terms in the integrand given above. As opposed to obtaining an integral series for the unknown density function μ by iteration, we determine the exact expression for the dipole density function by taking the partial Fourier transform of self-consistent relation given by the equation (3.10) and of the Green's function in momentum space provided by the equation (3.5), thus solving the equation exactly. We refer the readers to the Appendix for the details. We find the exact expression of the dipole density function

$$\mu(k_x, y') = -\left(\frac{1}{2}\sigma_3 + \frac{\partial G_0(k_x, y)}{\partial y}\bigg|_{y=0}\right)^{-1} G_0(k_x, y'). \tag{3.18}$$

where we evaluate the derivative term on the boundary $y_\alpha = y_\beta = 0$.

We substitute this expression into the equation (3.17) to obtain:

$$\delta\rho(k_x,\bar{E}) = \frac{1}{\pi}\,\mathrm{Im}\left\{\mathrm{Tr}_\sigma \int_0^\infty \mathrm{d}y\, \frac{\partial G_0(k_x,y)}{\partial y}\left(\frac{1}{2}\sigma_3 + \frac{\partial G_0(k_x,y)}{\partial y_\alpha}\Big|_{y=0}\right)^{-1} G_0(k_x,y)\right\}. \tag{3.19}$$

We refer the readers to the Appendix for the entire integrand.

This is the spectral function than contains the information about the boundary effects on the density of states for a smooth (nearly flat) boundary.

The recipe for carrying out the calculation is straightforward. First, we determine the free-space Green's function G_0 given in the equation (3.5) in mixed representation by the relation (3.16). Next, we determine the derivative of G_0 in mixed representation and we calculate $\partial_y G_0(k_x,y)|_{y=0}$. Finally, we substitute all the expressions into the equation (3.19). Then we carry out the trace over matrix Tr_σ and evaluate y-integral. Imaginary part of the resulting expression multiplied by $-\frac{1}{\pi}$ is the spectral function.

We find the exact formula for the edge corrections to the quasiparticle density of states for a chiral p-wave superconductor by following the recipe above.

We take partial Fourier transform of equation (3.5). In mixed representation, the free-space Green's function is

$$\begin{aligned} G_0(k_x,y-y') = \frac{\bar{E}\sigma_0 + 2k_\alpha k_x\sigma_1 - 2k_\alpha^2\sigma_3}{k_+^2 - k_-^2}\,(g_+ - g_-) \\ + \frac{1}{2}\sigma_3\,(g_+ + g_-) - \frac{2ik_\alpha\sigma_2}{k_+^2 - k_-^2}\,(\partial_y g_+ - \partial_y g_-)\,. \end{aligned} \tag{3.20}$$

where $g_\pm$ are

$$g_\pm = \frac{e^{-a_\pm|y-y'|}}{2a_\pm} \quad \text{and} \quad \mathrm{Re}\{a_\pm\} > 0. \tag{3.21}$$

where $a_\pm^2 = k_x^2 - k_\pm^2$ and $k_\pm^2 = \mu - 2k_\alpha^2 \pm \sqrt{4k_\alpha^4 + \bar{E}^2 - 4\mu k_\alpha^2}$. We refer the readers to the Appendix for the details of the calculation. We now substitute the expression for G_0 into the equation (3.19), and we carry out the rest of the operations on Mathematica © software [29]. We thus obtain the edge corrections to the density of states $\delta\rho(k_x,E)$ as a function of E and k_x. We present the resulting density plot of $\delta\rho(k_x,E)$ in Fig 3.2.

The system we work on exhibit particle-hole symmetry with broken time-reversal symmetry, that amount to $\mathbb{Z}$ classification in two dimensions with Chern number being 1. Considering the Chern number signals the number of gapless edge states in a system, the expectation was to have precisely one chiral edge state, a Majorana mode for $\mu > 0$ and no edge state (Chern number zero) for $\mu < 0$.

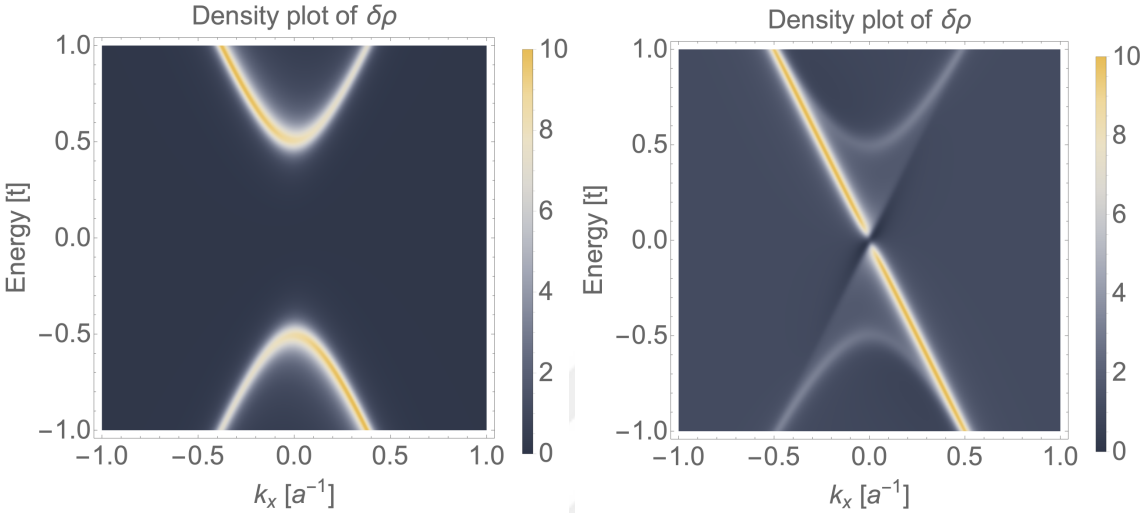

(a) $\mu = -0.5t$ (b) $\mu = 0.5t$

Figure 3.2 Density plot of the spectral function displaying the chiral Majorana mode in topologically non trivial phase $\mu > 0$, and no modes in topologically trivial phase $\mu < 0$

The density plot of $\delta\rho(k_x, \bar{E})$ exhibits the signatures of the topological nature of the system with a chiral edge state when $\mu > 0$. We observe the edge state crossing the Fermi energy with a negative group velocity ($\frac{\mathrm{d}E}{\mathrm{d}k_x} < 0$), therefore we identify it as a mode moving leftwards. Considering only allowed propagating direction along the boundary is left, the edge mode is chiral. Consequently, the quasiparticles cannot backscatter even in the presence of defects, as right propagation is not allowed.

Notice that the edge state is present only if $\mu > 0$. That is because the system is in the topologically non-trivial phase only if $\mu > 0$. Moreover, as discussed in Chapter 2, due to the superconducting nature of this system, the edge state we present here is, in fact, a Majorana mode.

To summarize, we demonstrated the existence of chiral Majorana modes for a bounded chiral p-wave superconductor in two dimensions in an analytical fashion by using multiple reflection expansion.

4 CONCLUSION

In this thesis, we calculated the flat boundary corrections of the density of states for a two-dimensional chiral p-wave superconductor. To this end, we used semiclassical methods to derive a spectral function that displays the existence of chiral Majorana edge modes. We used the method of multiple reflection expansion to calculate the boundary corrections to the DOS of this system and showed the signatures of Majorana modes with a novel technique. In the end, the analytical result we obtained displayed the properties of the system, especially the edge states present in the system due to its non-trivial topological nature.

Bibliography

[1] R. Balian and C. Bloch. Distribution of eigenfrequencies for the wave equation in a finite domain : I. three-dimensional problem with smooth boundary surface. *Annals of Physics*, 1970.

[2] J. Wurm, K. Richter, and İ. Adagideli. Edge effects in graphene nanostructures: From multiple reflection expansion to density of states. *Physical Review B*, 84(7), Aug 2011.

[3] İ. Adagideli and P. M. Goldbart. Quantal Andreev billiards: Semiclassical approach to mesoscale oscillations in the density of states. *International Journal of Modern Physics B*, 16(10):1381–1458, Apr 2002.

[4] E. N. Economou. *Green's Functions in Quantum Physics*. Berlin:Springer, 2006.

[5] J. D. Jackson. *Classical electrodynamics; 2nd ed.* Wiley, New York, NY, 1975.

[6] O. Kellogg. *Foundations of Potential Theory*. Springer Berlin Heidelberg, Berlin, Heidelberg, 1967.

[7] M. Sato and Y. Ando. Topological superconductors: a review. *Reports on Progress in Physics*, 80(7):076501, May 2017.

[8] J. F. Annett. *Superconductivity, superfluids and condensates*. Oxford master series in condensed matter physics. Oxford Univ. Press, Oxford, 2004.

[9] N. Read and D. Green. Paired states of fermions in two dimensions with breaking of parity and time-reversal symmetries and the fractional quantum Hall effect. *Physical Review B*, 61(15):10267–10297, Apr 2000.

[10] A. Altland and M. R. Zirnbauer. Nonstandard symmetry classes in mesoscopic normal-superconducting hybrid structures. *Physical Review B*, 55(2):1142–1161, Jan 1997.

[11] S. Ryu, A. P. Schnyder, A. Furusaki, and A. W. W. Ludwig. Topological insulators and superconductors: tenfold way and dimensional hierarchy. *New Journal of Physics*, 12(6):065010, Jun 2010.

[12] Y. Hatsugai. Chern number and edge states in the integer quantum Hall effect. *Phys. Rev. Lett.*, 71:3697–3700, Nov 1993.

[13] C. Caroli, P.G. De Gennes, and J. Matricon. Bound fermion states on a vortex line in a type ii superconductor. *Physics Letters*, 9(4):307–309, 1964.

[14] G. E. Volovik. Fermion zero modes on vortices in chiral superconductors. *Journal of Experimental and Theoretical Physics Letters*, 70(9):609–614, Nov 1999.

[15] A. Y. Kitaev. Unpaired Majorana fermions in quantum wires. *Physics-Uspekhi*, 44(10S):131–136, Oct 2001.

[16] J. Alicea, Y. Oreg, G. Refael, F. von Oppen, and Matthew P. A. Fisher. Non-abelian statistics and topological quantum information processing in 1d wire networks. *Nature Physics*, 7(5):412–417, Feb 2011.

[17] C. W. J. Beenakker, P. Baireuther, Y. Herasymenko, İ. Adagideli, L. Wang, and A. R. Akhmerov. Deterministic creation and braiding of chiral edge vortices. *Phys. Rev. Lett.*, 122:146803, Apr 2019.

[18] C. Bergemann, A. P. Mackenzie, S. R. Julian, D. Forsythe, and E. Ohmichi. Quasi-two-dimensional Fermi liquid properties of the unconventional superconductor sr2ruo4. *Advances in Physics*, 52(7):639–725, 2003.

[19] A. P. Mackenzie and Y. Maeno. The superconductivity of Sr_2RuO_4 and the physics of spin-triplet pairing. *Rev. Mod. Phys.*, 75:657–712, May 2003.

[20] L. Fu and C. L. Kane. Superconducting proximity effect and Majorana fermions at the surface of a topological insulator. *Phys. Rev. Lett.*, 100:096407, Mar 2008.

[21] L. Jiang, D. Pekker, J. Alicea, G. Refael, Y. Oreg, and F. von Oppen. Unconventional Josephson signatures of Majorana bound states. *Phys. Rev. Lett.*, 107:236401, Nov 2011.

[22] C. J. Bolech and E. Demler. Observing Majorana bound states in p-wave superconductors using noise measurements in tunneling experiments. *Phys. Rev. Lett.*, 98:237002, Jun 2007.

[23] E. Grosfeld, B. Seradjeh, and S. Vishveshwara. Proposed Aharonov-Casher interference measurement of non-Abelian vortices in chiral p-wave superconductors. *Phys. Rev. B*, 83:104513, Mar 2011.

[24] M. Z. Hasan and C. L. Kane. Colloquium: Topological insulators. *Reviews of Modern Physics*, 82(4):3045–3067, Nov 2010.

[25] C. Kallin and J. Berlinsky. Chiral superconductors. *Reports on Progress in Physics*, 79(5):054502, Apr 2016.

[26] X.-L. Qi and S.-C. Zhang. Topological insulators and superconductors. *Reviews of Modern Physics*, 83(4):1057, 2011.

[27] I. S. Gradshteyn and I. M. Ryzhik. *Table of integrals, series, and products.* Elsevier/Academic Press, Amsterdam, seventh edition, 2007. Translated from the Russian, Translation edited and with a preface by Alan Jeffrey and Daniel Zwillinger, With one CD-ROM (Windows, Macintosh and UNIX).

[28] H. Weyl. Ausbreitung elektromagnetischer wellen über einem ebenen leiter. *Annalen der Physik*, 365(21):481–500, 1919.

[29] Wolfram Research Inc. Mathematica, version 12.0. Champaign, IL, 2019.

[30] M. V. Berry. Quantal phase factors accompanying adiabatic changes. *Proceedings of the Royal Society of London. A. Mathematical and Physical Sciences*, 392(1802):45–57, 1984.

[31] M. Nakahara. *Geometry, topology and physics.* Graduate student series in physics. Hilger, Bristol, 1990.

[32] B. I. Halperin. Quantized Hall conductance, current-carrying edge states, and the existence of extended states in a two-dimensional disordered potential. *Phys. Rev. B*, 25:2185–2190, Feb 1982.

[33] S. M. Girvin. The quantum Hall effect: Novel excitations and broken symmetries. In A. Comtet, T. Jolicœur, S. Ouvry, and F. David, editors, *Aspects topologiques de la physique en basse dimension. Topological aspects of low dimensional systems*, pages 53–175, Berlin, Heidelberg, 1999. Springer Berlin Heidelberg.

[34] X.-L. Qi, T. L. Hughes, and S.-C. Zhang. Chiral topological superconductor from the quantum Hall state. *Phys. Rev. B*, 82:184516, Nov 2010.

[35] F. Wilczek. Majorana returns. *Nature Physics*, 5(9):614–618, 2009.

[36] A. Haim and Y. Oreg. Time-reversal-invariant topological superconductivity, 2018.

[37] F. D. M. Haldane. Model for a quantum Hall effect without Landau levels: Condensed-matter realization of the "parity anomaly". *Phys. Rev. Lett.*, 61:2015–2018, Oct 1988.

[38] D. Xiao, M.-C. Chang, and Q. Niu. Berry phase effects on electronic properties. *Reviews of Modern Physics*, 82(3):1959–2007, Jul 2010.

[39] J. Wang and S.-C. Zhang. Topological states of condensed matter. *Nature Materials*, 16(11):1062–1067, 2017.

[40] J. E. Moore. The birth of topological insulators. *Nature*, 464(7286):194–198, 2010.

[41] E. H. Hall. On a new action of the magnet on electric currents. *American Journal of Mathematics*, 2(3):287–292, 1879.

[42] D. J. Thouless, M. Kohmoto, M. P. Nightingale, and M. den Nijs. Quantized Hall conductance in a two-dimensional periodic potential. *Phys. Rev. Lett.*, 49:405–408, Aug 1982.

[43] K. v. Klitzing. Developments in the quantum Hall effect. *Philosophical Transactions of the Royal Society A: Mathematical, Physical and Engineering Sciences*, 363(1834):2203–2219, 2005.

[44] J. J. Sakurai. *Modern quantum mechanics; rev. ed.* Addison-Wesley, Reading, MA, 1994.

[45] J. Nilsson, A. R. Akhmerov, and C. W. J. Beenakker. Splitting of a Cooper pair by a pair of Majorana bound states. *Phys. Rev. Lett.*, 101:120403, Sep 2008.

[46] E. P. Wigner. On the statistical distribution of the widths and spacings of nuclear resonance levels. *Mathematical Proceedings of the Cambridge Philosophical Society*, 47(4):790–798, 1951.

[47] F. J. Dyson. The threefold way. algebraic structure of symmetry groups and ensembles in quantum mechanics. *Journal of Mathematical Physics*, 3(6):1199–1215, 1962.

[48] Y. E. Kraus, A. Auerbach, H. A. Fertig, and S. H. Simon. Majorana fermions of a two-dimensional $p_x + ip_y$ superconductor. *Phys. Rev. B*, 79:134515, Apr 2009.

[49] S. Das Sarma, C. Nayak, and S. Tewari. Proposal to stabilize and detect half-quantum vortices in strontium ruthenate thin films: Non-abelian braiding statistics of vortices in a $p_x + ip_y$ superconductor. *Phys. Rev. B*, 73:220502, Jun 2006.

[50] B. Pekerten, A. M. Bozkurt, and Adagideli I. Fermion parity switches of the ground state of Majorana billiards. *Phys. Rev. B*, 100:235455, Dec 2019.

[51] D. Tong. Lectures on the quantum Hall effect, 2016.

[52] J. Alicea. New directions in the pursuit of Majorana fermions in solid state systems. *Reports on Progress in Physics*, 75(7):076501, Jun 2012.

[53] K. v. Klitzing, G. Dorda, and M. Pepper. New method for high-accuracy determination of the fine-structure constant based on quantized Hall resistance. *Phys. Rev. Lett.*, 45:494–497, Aug 1980.

[54] C.W.J. Beenakker. Search for Majorana fermions in superconductors. *Annual Review of Condensed Matter Physics*, 4(1):113–136, 2013.

Appendix A

DERIVATION OF $G_0(k_x, y)$

The Green's function satisfies the equation

$$\left(\hat{H} - E\right) G_0(\mathbf{r}, \mathbf{r}; E) = \frac{\hbar^2}{2m}\delta(\mathbf{r} - \mathbf{r}'), \tag{A.1}$$

where the Hamiltonian descibes the quasiparticle dynamics for p-wave superconductors. It is given by

$$\hat{H} = (\frac{p^2}{2m} - \mu)\sigma_3 + \Delta\mathbf{p}\cdot\sigma. \tag{A.2}$$

We insert the expression for the hamiltonian into the equation and multiply both sides by $\frac{2m}{\hbar^2}$. Now the equation becomes:

$$\left[\frac{2m}{\hbar^2}(\frac{p^2}{2m} - \mu)\sigma_3 + \frac{2m\Delta}{\hbar^2}\mathbf{p}\cdot\sigma - \frac{2mE}{\hbar^2}\right] G_0(\mathbf{r}, \mathbf{r}'; E) = \delta(\mathbf{r} - \mathbf{r}'). \tag{A.3}$$

To make it concise, we make new algebraic definitions as follows $\mathbf{k} = \frac{\mathbf{p}}{\hbar}$, $k_\alpha = \frac{m\Delta}{\hbar}$, $\mu = \frac{2m\mu}{\hbar^2}$, $\bar{E} = \frac{2mE}{\hbar^2}$.

The free space Green's function in momentum space is the formal inverse of the 2×2 matrix $(\hat{H}(\mathbf{k}) - E)$:

$$G_0(\mathbf{k}) = \left((k^2 - \mu)\sigma_3 + 2k_\alpha\mathbf{k}\cdot\sigma - \bar{E}\right)^{-1}. \tag{A.4}$$

We multiply both the numerator and the denominator by $\left(\bar{E}\sigma_0 + \hat{H}(\mathbf{k})\right)$, and additionally we define the constants $k_\pm^2 = \mu - 2k_\alpha^2 \pm \sqrt{4k_\alpha^4 + \bar{E}^2 - 4\mu k_\alpha^2}$. Finally free space Green's function in k space becomes:

$$\begin{aligned} G_0(\mathbf{k}) = {} & \frac{\bar{E} + 2k_\alpha k_x\sigma_1 - 2k_\alpha^2\sigma_3}{k_+^2 - k_-^2}\left(\frac{1}{k^2 - k_+^2} - \frac{1}{k^2 - k_-^2}\right) \\ & + \frac{1}{2}\sigma_3\left(\frac{1}{k^2 - k_+^2} + \frac{1}{k^2 - k_-^2}\right) + \frac{2k_\alpha\sigma_2}{k_+^2 - k_-^2}\left(\frac{k_y}{k^2 - k_+^2} - \frac{k_y}{k^2 - k_-^2}\right). \end{aligned} \tag{A.5}$$

We now evaluate the partial Fourier transformation of $G_0(\mathbf{k})$:

$$G_0(k_x, y-y') = \int \frac{\mathrm{d}k_y}{2\pi} e^{ik_y(y-y')} G_0(\mathbf{k}) \tag{A.6}$$

We first define the functions $a_\pm^2 = k_x^2 - k_\pm^2$ and $g_\pm(\mathbf{k}) = \frac{1}{k^2+a_\pm^2}$ which are present in G_0. We first take the partial Fourier transformations of $g_\pm$:

$$g_\pm(k_x, y-y') = \int_{-\infty}^{\infty} \frac{\mathrm{d}k_y}{2\pi} \frac{e^{ik_y(y-y')}}{k_y^2 + a_\pm^2} = \frac{e^{-a_\pm|y-y'|}}{2a_\pm}. \tag{A.7}$$

Here note that we pick the branch cuts such that $\mathrm{Re}\{a_\pm\} > 0$. Keeping this in mind, the whole expression becomes:

$$\begin{aligned} G_0(k_x, y-y') = \frac{\bar{E} + 2k_\alpha k_x \sigma_1 - 2k_\alpha^2 \sigma_3}{k_+^2 - k_-^2} (g_+ - g_-) \\ + \frac{1}{2}\sigma_3 (g_+ + g_-) - \frac{2ik_\alpha \sigma_2}{k_+^2 - k_-^2} (\partial_y g_+ - \partial_y g_-) \end{aligned} \tag{A.8}$$

The normal derivative $\partial_y G_0(k_x, y)$ is determined by taking the y-derivative of the above expression.

DERIVATION OF $\delta\rho(k_x, E)$

The main equation for the edge contributions in terms of k_x are written as :

$$\delta\rho = -\frac{1}{\pi} \mathrm{Im}\mathrm{Tr}\left[G_1(k_x, Y; E + i0^+)\right] \tag{A.9}$$

Here G_1 represents the boundary integral corresponding to edge corrections.

$$\delta\rho = -\tfrac{1}{\pi}\,\mathrm{Im}\Big\{\mathrm{Tr}_\sigma\Big[\int \mathrm{d}y \int \mathrm{d}y'\, \delta(y-y') \int \mathrm{d}x \int \mathrm{d}x'\, \delta(x-x') \int \mathrm{d}x_\alpha\, \tfrac{\partial G_0(\mathbf{r},\boldsymbol{\alpha})}{\partial y_\alpha} \mu(\boldsymbol{\alpha}, \mathbf{r}')\Big]\Big\} \tag{A.10}$$

We write the $\delta(x-x')$ explicitly as an integral in momentum space, and split its representation $e^{ik_x(x-x')}$ to express the functions in mixed form:

$$\delta\rho = -\frac{1}{\pi}\,\mathrm{Im}\Big\{\mathrm{Tr}_\sigma\Big[\int \mathrm{d}y \int \mathrm{d}y'\,\delta(y-y') \int \mathrm{d}x \int \mathrm{d}x' \int \mathrm{d}k_x\, e^{-ik_x(x_\alpha - x)} e^{-ik_x(x'-x_\alpha)} \int \mathrm{d}x_\alpha\, \frac{\partial G_0(x_\alpha - x, y_\alpha - y)}{\partial y_\alpha} \mu(x'-x_\alpha, y'-y_\alpha)\Big]\Big\} \tag{A.11}$$

These integrals can be interpreted as a partial Fourier transform convolution of two functions. Thus, in mixed representation the equation becomes

$$\delta\rho = -\frac{1}{\pi}\,\mathrm{Im}\left\{\mathrm{Tr}_\sigma\left[\int_{\text{length}} \mathrm{d}x \int \mathrm{d}k_x \int \mathrm{d}y\, \frac{\partial G_0(k_x, y_\alpha - y)}{\partial y_\alpha} \mu(k_x, y - y_\alpha)\right]_{y_\alpha=0}\right\} \tag{A.12}$$

We take the length integral, and express ρ in terms of k_x and E.

$$\delta\rho(k_x, E) = -\frac{|\ell|}{\pi}\,\mathrm{Im}\left\{\mathrm{Tr}_\sigma\left[\int \mathrm{d}y\, \frac{\partial G_0(k_x, y_\alpha - y)}{\partial y_\alpha} \mu(k_x, y - y_\alpha)\right]_{y_\alpha=0}\right\} \tag{A.13}$$

Here we note that, we set the system length term to unity.

DERIVATION OF $\mu(k_x, y)$

We are required to find the expression for the unknown density function in mixed representation. As mentioned, the boundary is smooth enough that we can take the partial Fourier transform along the boundary. We start from the self consistency relation that is defined on the boundary.

$$\frac{1}{2}\sigma_3 \mu(\boldsymbol{\beta}, \mathbf{r}') = -G_0(\boldsymbol{\beta}, \mathbf{r}') - \int_{\partial S} \mathrm{d}\sigma_\alpha\, \frac{\partial G_0(\mathbf{r}, \boldsymbol{\alpha})}{\partial \mathbf{n}_\alpha} \mu(\boldsymbol{\alpha}, \mathbf{r}'). \tag{A.14}$$

We take the partial Fourier transformation of both sides,

$$\begin{aligned}&\frac{1}{2}\sigma_3 \mu(k_x, y' - y_\beta) = -G_0(k_x, y' - y_\beta)\\ &-\int \mathrm{d}(x' - x_\beta)\, e^{-ik_x(x'-x_\beta)} \int \mathrm{d}x_\alpha\, \frac{\partial G_0(x_\alpha - x_\beta, y_\alpha - y_\beta)}{\partial y_\alpha}\bigg|_{y_\alpha = y_\beta = 0} \mu(x_\alpha - x', y' - y_\alpha)\end{aligned} \tag{A.15}$$

As mentioned $\boldsymbol{\alpha}$ and $\boldsymbol{\beta}$ are points on boundary, therefore $y_\alpha = y_\beta = 0$. Note that, this leads to the normal derivative of G_0 getting evaluated at the boundary, we simplify the variables to show clear presentation.

We separate $e^{-ik_x(x'-x_\beta)} = e^{-ik_x(x'-x_\alpha)}e^{-ik_x(x_\alpha-x_\beta)}$, then we group the integrals as,

$$\begin{aligned}&\frac{1}{2}\sigma_3\mu(k_x,y') = -G_0(k_x,y')\\&-\int \mathrm{d}(x'-x_\beta)\, e^{-ik_x(x_\alpha-x_\beta)}\left.\frac{\partial G_0(x_\alpha-x_\beta,y)}{\partial y}\right|_{y=0}\int \mathrm{d}x_\alpha\, e^{-ik_x(x'-x_\alpha)}\mu(x_\alpha-x',y').\end{aligned} \tag{A.16}$$

We identify the integral as a partial Fourier convolution of two functions. Finally, in mixed representation we write the self consistency relation for μ exactly for a flat boundary:

$$\mu(k_x,y') = -\left(\frac{1}{2}\sigma_3 - \left.\frac{\partial G_0(k_x,y)}{\partial y}\right|_{y=0}\right)^{-1} G_0(k_x,y'). \tag{A.17}$$

Finally this exact expression can replace the one in the relation for $\delta\rho$.

THE CORRECTION GREEN'S FUNCTION

$$\begin{aligned}G_1 = &\left(\frac{\bar{E}+2k_\alpha k_x\sigma_1-2k_\alpha^2\sigma_3}{k_+^2-k_-^2}(a_+g_+-a_-g_-)+\frac{1}{2}\sigma_3(a_+g_++a_-g_-)-\frac{2ik_\alpha\sigma_2}{k_+^2-k_-^2}(a_+^2g_+-a_-^2g_-)\right)\\&\left(\frac{1}{2}\sigma_3+\frac{ik_\alpha}{k_+^2-k_-^2}(a_+-a_-)\sigma_2\right)^{-1}\\&\left(\frac{\bar{E}+2k_\alpha k_x\sigma_1-2k_\alpha^2\sigma_3}{k_+^2-k_-^2}(g_+-g_-)+\frac{1}{2}\sigma_3(g_++g_-)-\mathrm{sgn}(y)\frac{2ik_\alpha\sigma_2}{k_+^2-k_-^2}(g_+-g_-)\right)\end{aligned} \tag{A.18}$$

where $g_\pm$ is given by (A.7), $a_\pm^2 = k_x^2 - k_\pm^2$ and $k_\pm^2 = \mu - 2k_\alpha^2 \pm \sqrt{4k_\alpha^4 + \bar{E}^2 - 4\mu k_\alpha^2}$.